Exact-exchange-based quasiparticle calculations

Wilfried G. Aulbur,[1] Martin Städele,[2] and Andreas Görling[3]
[1]*Department of Physics, Ohio State University, Columbus, Ohio 43210*
[2]*Department of Physics, University of Illinois at Urbana-Champaign, Illinois 61801*
[3]*Lehrstuhl für Theoretische Chemie, Technische Universität München, D-85748 Garching, Germany*
(Received 15 September 1999; revised manuscript received 1 February 2000)

One-particle wave functions and energies from Kohn-Sham calculations with the exact local Kohn-Sham exchange and the local density approximation (LDA) correlation potential [EXX(c)] are used as input for quasiparticle calculations in the *GW* approximation (GWA) for eight semiconductors. Quasiparticle corrections to EXX(c) band gaps are small when EXX(c) band gaps are close to experiment. In the case of diamond, quasiparticle calculations are essential to remedy a 0.7 eV underestimate of the experimental band gap within EXX(c). The accuracy of EXX(c)-based GWA calculations for the determination of band gaps is as good as the accuracy of LDA-based GWA calculations. For the lowest valence band width a qualitatively different behavior is observed for medium- and wide-gap materials. The valence band width of medium- (wide-) gap materials is reduced (increased) in EXX(c) compared to the LDA. Quasiparticle corrections lead to a further reduction (increase). As a consequence, EXX(c)-based quasiparticle calculations give valence band widths that are generally 1–2 eV smaller (larger) than experiment for medium- (wide-) gap materials.

I. INTRODUCTION

The description of excited states in solids is a challenging and important problem in condensed matter physics since excited states are needed to determine transport and optical properties of materials. Until the mid-1980s, a commonly used way to determine, for example, band structures of materials was based on density functional theory in the Kohn-Sham formulation using the local density approximation (LDA).[1,2] This approach maps the many-body problem onto a system of noninteracting, fictitious Kohn-Sham particles. Within the original formulation of Kohn-Sham theory, the eigenvalues of the single-particle Kohn-Sham equations are pure auxiliary quantities without physical meaning. Only the energy of the highest occupied Kohn-Sham orbital can be rigorously related to the ionization energy of electronic systems. Recent work provides evidence that Kohn-Sham eigenvalue differences are well-defined approximations to excitation energies.[3,4] Indeed, Kohn-Sham band structures compare rather well with experiment. The most notable exception is the band gap of insulators, which is generally 0.5–2.0 eV smaller than experimental values.

The discrepancy between experimental and Kohn-Sham energy gaps has stimulated significant theoretical work. Perdew and Levy[5] and Sham and Schlüter[6] pointed out that the discontinuity in the exchange-correlation potential Δ_{xc} upon addition of one electron to an insulator with completely filled valence bands accounts for the discrepancy between the single-particle Kohn-Sham band gap ε_{gap}^{KS} and experiment,

$$E_{gap}=\varepsilon_{gap}^{KS}+\Delta_{xc}=\varepsilon_{gap}^{LDA}+\Delta\varepsilon_{gap}^{LDA}+\Delta_{xc}. \qquad (1)$$

While the sum of the error $\Delta\varepsilon_{gap}^{LDA}$ of the LDA band gap ε_{gap}^{LDA} and the discontinuity Δ_{xc} is large, there is a controversy about the magnitude of the individual terms $\Delta\varepsilon_{gap}^{LDA}$ and Δ_{xc}. According to the work of Godby, Schlüter, and Sham[7] Δ_{xc} is large in semiconductors. In model systems, on the other hand, Δ_{xc} is reported to be large in some cases while it is determined to be small for others.

Very recently, new density functional methods have been presented in the literature whose energy gaps generally agree much better with experiment than those of the LDA (for a review see, for instance, Ref. 10). In one such approach, which has been studied in much detail for semiconductors, all exchange-related quantities are computed exactly.[11–13] This ''EXX method'' allows the determination of the exact local Kohn-Sham exchange potential and generalizes the optimized effective potential method[14]—commonly used for atoms—to solids. In particular, self-interaction errors due to incomplete cancellation of the self-Hartree and the self-exchange potentials are completely eliminated in exact-exchange density functional theory. Combination of exact Kohn-Sham exchange with LDA or generalized gradient approximations (GGA) for correlation leads for standard semiconductors to energy gaps and structural properties that agree well with experiment.

An alternative way to describe the excited states of materials is provided by computational many-body theory using the dynamically screened or *GW* approximation (GWA). In the GWA, the electronic self-energy, which describes exchange and correlation beyond the Hartree approximation, is expressed as the product of a single-particle propagator *G* and a screened interaction *W* (for recent reviews of the GWA, see Refs. 10 and 15). In principle, the GWA requires the self-consistent solution of a set of four coupled integral equations as will be discussed in more detail below. GWA calculations that are (i) non-self-consistent, (ii) use LDA energies and wave functions as input, and (iii) neglect the imaginary part of the self-energy describe the experimental electronic structure of *sp* bonded semiconductors and insulators generally to within 0.1–0.5 eV.[10]

In this work we use orbitals and eigenvalues from a self-consistent calculation with the exact local KS exchange potential and the LDA correlation potential as input for the

GWA calculations. This approach is evaluated here for eight semiconductors (Si, Ge, C, SiC, GaAs, AlAs, GaN, and AlN). An application of the method for *d* and *f* electrons is left for a future study.

II. METHODOLOGY

This section summarizes important equations for both the EXX method and the GWA approach. For further details we refer the reader to Refs. 11 (exact exchange) and 10 (GWA).

A. Exact-exchange density functional theory

In the Kohn-Sham formalism of density functional theory a set of single-particle Kohn-Sham equations[16] is solved,

$$\left(-\frac{\nabla^2}{2}+V_{KS}([\rho];\mathbf{r})\right)\Phi_{n\mathbf{k}}(\mathbf{r})=\varepsilon_{n\mathbf{k}}\Phi_{n\mathbf{k}}(\mathbf{r}), \tag{2}$$

where n is a band index, $\mathbf{k}$ is a wave vector in the first Brillouin zone, and $\Phi_{n\mathbf{k}}$ and $\varepsilon_{n\mathbf{k}}$ are the wave function and the eigenvalue of the ficticious Kohn-Sham particle. The Kohn-Sham potential V_{KS} is the sum of the external (ionic) potential V_{ext}, the Hartree potential V_H, the exchange potential V_X, and the correlation potential V_C:

$$V_{KS}([\rho];\mathbf{r})=V_{ext}(\mathbf{r})+V_H([\rho];\mathbf{r})+V_X([\rho];\mathbf{r})+V_C([\rho];\mathbf{r}). \tag{3}$$

All potentials are functionals of the ground state density $\rho(\mathbf{r})$,

$$\rho(\mathbf{r})=2\sum_{v\mathbf{k}}|\Phi_{v\mathbf{k}}(\mathbf{r})|^2. \tag{4}$$

The factor 2 accounts for spin degeneracy and the sum runs over all occupied states in the first Brillouin zone. Since, the KS potential is a functional of the density functional of the density, Eqs. (2) and (4) have to be solved self-consistently.

Exact-exchange density functional calculations determine the exchange energy according to its definition as

$$E_X[\rho]=-\frac{1}{2}\sum_{v,v'}\sum_{\mathbf{k},\mathbf{k}'}\int\int\frac{\Phi^*_{v\mathbf{k}}(\mathbf{r})\Phi_{v\mathbf{k}}(\mathbf{r}')\Phi_{v'\mathbf{k}'}(\mathbf{r}')\Phi^*_{v'\mathbf{k}'}(\mathbf{r})}{|\mathbf{r}-\mathbf{r}'|}d\mathbf{r}d\mathbf{r}'. \tag{5}$$

The $\Phi_{v\mathbf{k}}$ are occupied Kohn-Sham orbitals (i.e., in pseudopotential schemes the valence Kohn-Sham orbitals).[17] The exact local Kohn-Sham exchange potential is defined as

$$V_X([\rho];\mathbf{r})=\left.\frac{\delta E_X[\rho]}{\delta\rho(\mathbf{r})}\right|_{\rho(\mathbf{r})=\rho_0(\mathbf{r})} \tag{6}$$

with $\rho_0(\mathbf{r})$ being the ground state electron density. Usage of the chain rule for functional derivatives leads to

$$\begin{aligned}V_X([\rho];\mathbf{r})&=\frac{\delta E_X[\rho]}{\delta\rho(\mathbf{r})}\\&=\sum_{v,\mathbf{k}}\int\int\left(\frac{\delta E_X[\rho]}{\delta\Phi_{v\mathbf{k}}(\mathbf{r}')}\frac{\delta\Phi_{v\mathbf{k}}(\mathbf{r}')}{\delta V_{KS}(\mathbf{r}'')}+\text{c.c.}\right)\\&\quad\times\frac{\delta V_{KS}(\mathbf{r}'')}{\delta\rho(\mathbf{r})}d\mathbf{r}'d\mathbf{r}''.\end{aligned} \tag{7}$$

In the above equation, one determines $\delta E_X/\delta\Phi_{n\mathbf{k}}$ from Eq. (5), $\delta\Phi_{v\mathbf{k}}/\delta V_{KS}$ is given by first-order perturbation theory, and $\delta V_{KS}/\delta\rho$ is the inverse independent-particle polarizability [see Eq. (16); $\mathbf{G}=\mathbf{0}$ terms are excluded in the inversion]. In most applications of exact-exchange density functional theory, correlation is included on the level of the LDA or GGA.

Exact-exchange plus LDA or GGA correlation calculations have a number of advantages compared to standard LDA calculations. The theory is largely self-interaction-free which may lead to a better description of localized electronic states than in the LDA.[18] In addition, the exact-exchange potential decays correctly as $-1/r$ for finite systems at large distances r rather than exponentially as is the case in the LDA. The ionization energy of finite systems and the description of atomic Rydberg spectra are thus greatly improved in EXX(c) compared to the LDA. Significant improvements in the description of, for instance, metal surfaces are likely, although explicit calculations have not been carried out yet.

B. Quasiparticle calculations

A successful approximation for the determination of excited states is based on the quasiparticle concept and the Green function method. The behavior of the quasiparticle wave function $\Psi_{n\mathbf{k}}$ and energy $\varepsilon_{n\mathbf{k}}$ is governed by

$$\begin{aligned}&\left(-\frac{1}{2}\nabla^2+V_H+V_{ext}\right)\Psi_{n\mathbf{k}}(\mathbf{r})+\int\Sigma(\mathbf{r},\mathbf{r}';E_{n\mathbf{k}})\Psi_{n\mathbf{k}}(\mathbf{r}')d\mathbf{r}'\\&\quad=E_{n\mathbf{k}}\Psi_{n\mathbf{k}}(\mathbf{r}).\end{aligned} \tag{8}$$

Here $\Psi_{n\mathbf{k}}$ and $E_{n\mathbf{k}}$ are the quasiparticle wave function and energy, respectively.

The central object of the Green function method is the quasiparticle self-energy Σ, a non-Hermitian, energy-dependent, nonlocal operator that describes exchange and correlation effects beyond the Hartree approximation. A determination of the self-energy can only be approximate and a working scheme for the quantitative calculation of excitation energies in metals, semiconductors, and insulators is the so-called dynamically screened or GW approximation.

In principle, the GWA requires a self-consistent solution of a set of coupled integral equations that link the self-energy

Σ, the Green function G, the irreducible polarizability P, the screened interaction W, and the bare Coulomb interaction v:

$$\Sigma(1,2)=iG(1,2)W(1^+,2), \tag{9}$$

$$W(1,2)=v(1,2)+\int W(1,3)P(3,4)v(4,2)d(3,4), \tag{10}$$

$$P(1,2)=-iG(1,2)G(2,1). \tag{11}$$

Here $1=(\mathbf{r},\sigma,t)$, $1^+=(\mathbf{r},\sigma,t+\delta)$, $\delta>0$ and infinitesimal, is a combined space, spin, and time vector. We neglect the explicit spin dependence in what follows. The above set of simplified Hedin equations[19,20] is closed by Dyson's equation (E = energy),

$$G(\mathbf{r},\mathbf{r}';E)=G^0(\mathbf{r},\mathbf{r}';E)+\int\int G^0(\mathbf{r},\mathbf{r_1};E) \times\Sigma(\mathbf{r_1},\mathbf{r_2};E)G(\mathbf{r_2},\mathbf{r}';E)d\mathbf{r_1}d\mathbf{r_2}, \tag{12}$$

in which G^0 is the independent-particle propagator. The self-consistency cycle is schematically shown in Fig. 1.

In practice, the self-energy Σ is often evaluated non-self-consistently using the independent-particle Green function G^0,

$$G^0(\mathbf{r},\mathbf{r}';E)=\sum_{n,\mathbf{k}}\frac{\Phi_{n\mathbf{k}}(\mathbf{r})\Phi^*_{n\mathbf{k}}(\mathbf{r}')}{E-\varepsilon_{n,\mathbf{k}}}, \tag{13}$$

in Eq. (9). Here G^0 can be, for example, the LDA, Hartree-Fock, or as in the present case, the EXX(c) independent-particle propagator. The screened interaction W in Eq. (9) is determined in the random-phase approximation (RPA), that is,

$$W_{\mathbf{GG}'}(\mathbf{q};\omega)=\frac{4\pi}{|\mathbf{q}+\mathbf{G}|^2}(\varepsilon^{RPA}_{\mathbf{GG}'})^{-1}(\mathbf{q};\omega), \tag{14}$$

where ω is the frequency of the screened interaction, $\mathbf{q}$ is a vector in the first Brillouin zone, and $\mathbf{G}$ and $\mathbf{G}'$ are reciprocal lattice vectors. The frequency dependence of the RPA dielectric matrix $\varepsilon^{RPA}_{\mathbf{GG}'}(\mathbf{q},\omega)$ is in this work approximated by a plasmon pole model[21] and its $\omega=0$ value determined using the independent-particle polarizability $P^0_{\mathbf{GG}'}(\mathbf{q})$ via

$$\varepsilon^{RPA}_{\mathbf{GG}'}(\mathbf{q};\omega)=\delta_{\mathbf{GG}'}-\frac{4\pi}{|\mathbf{q}+\mathbf{G}|^2}P^0_{\mathbf{GG}'}(\mathbf{q};\omega). \tag{15}$$

The latter is given by the Adler-Wiser formalism[22–24]

$$P^0_{\mathbf{GG}'}(\mathbf{q})=\frac{4}{V}\sum_{v,c}\sum_{\mathbf{k}}^{BZ}\frac{M^{vc}_{\mathbf{G}}(\mathbf{k},\mathbf{q})[M^{vc}_{\mathbf{G}'}(\mathbf{k},\mathbf{q})]^*}{\varepsilon_{v,\mathbf{k}-\mathbf{q}}-\varepsilon_{c,\mathbf{k}}}, \tag{16}$$

where V is the crystal volume, the sums are over valence (v) or conduction (c) bands or over the first Brillouin zone, and $\varepsilon_{v,\mathbf{k}-\mathbf{q}}$ and $\varepsilon_{c\mathbf{k}}$ are as in Eq. (13). The matrix elements $M^{vc}_{\mathbf{G}}(\mathbf{k},\mathbf{q})$ are defined as

$$M^{vc}_{\mathbf{G}}(\mathbf{k},\mathbf{q})=\int\Phi^*_{v,\mathbf{k}-\mathbf{q}}(\mathbf{r})e^{-i(\mathbf{q}+\mathbf{G})\cdot\mathbf{r}}\Phi_{c\mathbf{k}}(\mathbf{r})d\mathbf{r}. \tag{17}$$

With $\omega_p(\mathbf{q})$ as plasmon eigenvalues and $\Theta_{p\mathbf{q}}(\mathbf{G})$ as suitably scaled coefficients of the plasmon eigenfunctions[10] the exchange (Σ^X) and energy-dependent correlation [$\Sigma^C(E)$] parts of the self-energy can be determined as[16] [$\langle\mathbf{r}|m,\mathbf{k}\rangle\equiv\Phi_{m\mathbf{k}}(\mathbf{r})$]

$$\langle m,\mathbf{k}|\Sigma^X|l,\mathbf{k}\rangle=-\frac{4\pi}{V}\sum_{v}^{occ}\sum_{\mathbf{q}}^{BZ}\sum_{\mathbf{G}}\frac{M^{vl}_{\mathbf{G}}(\mathbf{k},\mathbf{q})[M^{vm}_{\mathbf{G}}(\mathbf{k},\mathbf{q})]^*}{|\mathbf{q}+\mathbf{G}|^2}, \tag{18}$$

$$\langle m,\mathbf{k}|\Sigma^C(E)|l,\mathbf{k}\rangle=\frac{1}{V}\sum_{\mathbf{q}}^{BZ}\sum_{n}^{occ+unocc}\sum_{p}^{PPM}\frac{\beta^{nm}_p(\mathbf{k},\mathbf{q})[\beta^{nl}_p(\mathbf{k},\mathbf{q})]^*}{E-\varepsilon_{n\mathbf{k}-\mathbf{q}}+\omega_p(\mathbf{q})\mathrm{sgn}(\mu-\varepsilon_{n\mathbf{k}-\mathbf{q}})}, \tag{19}$$

where the matrix elements are defined as

$$\beta^{nm}_p(\mathbf{k},\mathbf{q})=\sum_{\mathbf{G}}[M^{nm}_{\mathbf{G}}(\mathbf{k},\mathbf{q})]^*\Theta_{p\mathbf{q}}(\mathbf{G}). \tag{20}$$

C. Technical details

All calculations were carried out at the experimental lattice constants. The LDA and LDA-based GWA calculations use LDA Troullier-Martins pseudopotentials[25] in the Kleinman-Bylander form;[26] the EXX(c) and EXX(c)-based GWA calculations use semilocal EXX(c) Troullier-Martins pseudopotentials. We have checked that the use of different pseudopotentials does not significantly affect our results.[27] Nonlinear core corrections[28] were not used. The LDA correlation potentials use the Perdew-Zunger parametrization[29] of the Ceperley-Alder quantum Monte Carlo data.[30]

All numerical cutoffs are identical in the LDA and EXX(c) calculations. We use 10 special k points[31] to determine the ground state density, the dielectric matrix, and the self-energy corrections. We use an energy cutoff of 12.5 hartree for Si, Ge, GaAs, and AlAs; 22.5 hartree for GaN and AlN; 25 hartree for SiC; and 32.5 hartree for diamond.[32] We keep 196 conduction bands in the determination of the dielectric matrix for all materials and a reciprocal space cutoff of 3.6 a.u. (Si, Ge, GaAs, AlAs); 5.0 a.u. (GaN, AlN, SiC); or 6.0 a.u. (diamond).

The energy dependence of the dielectric matrix is approximated by the Engel-Farid plasmon pole model.[21] The number of bands retained in the sum over n in Eq. (19) is restricted to 200 for all materials except Si, for which 100

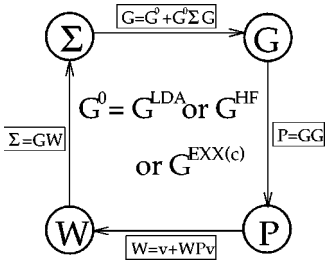

FIG. 1. Schematic representation of the self-consistent determination of the self-energy in the GWA. Entries in boxes symbolize the mathematical relations that link Σ, G, Γ, P, and W. P, W, and Σ are constructed, for example, starting from a LDA, Hartree-Fock, or EXX(c) independent-particle propagator. Subsequently, Σ updates the quasiparticle wave functions and energies and a new Green function G is determined. This process is repeated until self-consistency is reached. Most practical applications either determine only the quasiparticle energies self-consistently or do not update quasiparticle energies and wave functions at all.

bands are more than adequate for good convergence.[10] The reciprocal space cutoff used for the determination of the matrix elements in Eq. (20) is 3.4 a.u. (Si, Ge, GaAs, AlAs) or 4.5 a.u. (C, SiC, GaN, AlN). The number of plasmon pole bands summed over is 60 for Si, 100 for Ge, GaAs, and AlAs, and 120 for C, SiC, GaN, and AlN. Self-energy corrections are determined in first-order perturbation theory without updating the energies in the Green function.

III. RESULTS

A. Densities and potentials

Figures 2 and 3 show (i) the valence electron densities of an exact-exchange calculation with LDA correlation and of an LDA calculation (upper panel), and (ii) the exact exchange, the LDA exchange, and the LDA correlation potentials along the $\langle 111 \rangle$ direction in representative homopolar (Si and C, Fig. 2) and heteropolar (GaAs and GaN, Fig. 3) semiconductors. All potentials are evaluated at the EXX(c) density. Using LDA densities to evaluate the LDA exchange and correlation potentials does not significantly modify the shape of the potentials. Only minor quantitative changes ($<10\%$ of total potential variation) can be observed. In each case, we have chosen a medium-gap material (Si and GaAs) and a wide-gap material (C and GaN). The LDA correlation potential—used in both the LDA and the EXX(c) calculations—is smaller by a factor of about 10 than the exchange potentials and featureless on the scale of the plots.

The upper panels of Figs. 2 and 3 show that EXX(c) calculations concentrate more density in the bonding region than the LDA calculations. To understand this trend, the lower panels compare the exact-exchange and LDA exchange potentials. While the qualitative features of both potentials are similar, the exact-exchange potential is deeper in the bonding and shallower in the antibonding region than the LDA exchange potential. This behavior of the exact-exchange versus the LDA exchange potential is to be expected since (i) EXX(c) eliminates most of the self-interaction errors inherent to the LDA and thus allows a larger electron density in the bonds, (ii) self-interaction errors are larger for occupied than unoccupied states, and (iii)

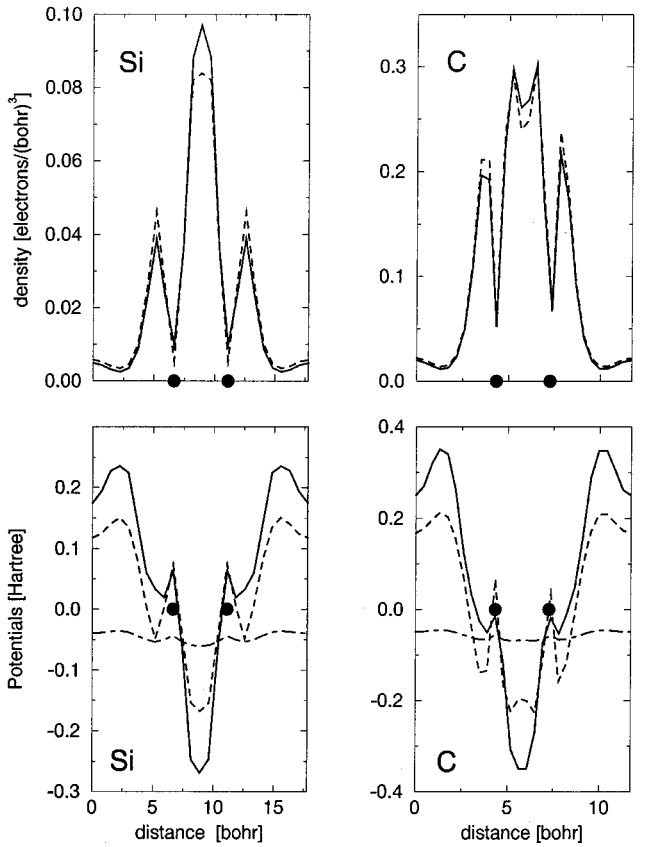

FIG. 2. EXX(c) (solid lines) and LDA (dashed lines) valence densities (upper panel) and exchange potentials (lower panel) for Si and C along the $\langle 111 \rangle$ direction. In lower panel dot-dashed line shows LDA correlation potential. Solid circles symbolize the positions of the Si and C atoms, respectively. The unit cell average of the exchange potentials is zero. EXX(c) eliminates self-interaction errors in regions of localized density such as the bonding region. This leads to a deeper potential in bonding regions where valence electrons are concentrated and opens up the EXX(c) band gap compared to the LDA.

self-interaction errors generally lead to LDA states that are underbound (several eV in the case of d and f electrons). Note that Hartree-Fock theory, which is self-interaction-free for occupied states, also leads to a stronger density localization compared to the LDA.[11,33]

Comparison of the exact-exchange and LDA exchange potentials in the lower panels of Figs. 2 and 3 suggests that, in a crude approximation, the potentials differ by two different constants attributed to two regions of space. In the bonding region—where the valence electrons are concentrated—the difference between the exact-exchange potential and the LDA exchange potential is *negative*. In the interstitial region—where the conduction electrons are concentrated—the difference is *positive*. Hence, one would expect that the bonding (occupied) and antibonding (unoccupied) LDA and EXX(c) wave functions that are located predominantly in one or the other region of space would be similar, i.e., have overlaps close to unity. Determination of the overlap integral $|\langle \Phi_{n\mathbf{k}}^{EXX(c)} | \Phi_{n\mathbf{k}}^{LDA} \rangle|$ for the 10 lowest states at the Γ, X, and L points in Si, C, GaAs, and GaN gives values that range between 0.9985 and 0.9999 for Si, 0.9987 and 0.9999 for diamond, 0.9808 and 0.9998 for GaAs, and 0.9973 and 0.9998

TABLE I. Comparison of Si LDA, LDA-based GWA (LDA+GWA), EXX(c), EXX(c)-based GWA (EXX+GWA), and experimental (italic) energies at the Γ, X, and L points. For ease of comparison, all valence band tops are set to zero. The calculations use pseudopotentials and plane waves, a plasmon pole model, and determine self-energy shifts in first-order perturbation theory. All energies are given in eV.

Method	Γ_{1v}	Γ'_{25v}	Γ_{15c}	Γ'_{2c}		
Expt.	$-12.5(6)$, [a] $-12.4(6)$ [b] -11.4, [p] -11.2 [q]	0.00	*3.34–3.36*, [c] *3.05*[d]	*4.15(5)*, [e] 4.1, [d] *4.21(2)*[f]		
LDA	−11.96	0.00	2.56	3.18		
LDA + GWA	−11.90	0.00	3.25	3.86		
EXX	−11.58	0.00	3.27	4.45		
EXX + GWA	−10.88	0.00	3.53	4.65		
	X_{1v}	X_{4v}	X_{1c}	X_{4c}		
Expt.		*−2.9*, [e] *−2.5(3)*, [a] *−3.3(2)*[i]	*1.13*, [g] *1.25*[d]			
LDA	−7.82	−2.87	0.66	9.99		
LDA + GWA	−7.90	−2.96	1.31	10.72		
EXX	−7.47	−2.61	1.51	11.14		
EXX + GWA	−7.29	−2.84	1.44	11.73		
	L'_{2v}	L_{1v}	L'_{3v}	L_{1c}	L_{3c}	L'_{2c}
Expt.	*−9.3(4)*[a]	*−6.8(2)*, [a] *−6.4(4)*[b]	*−1.2(2)*, [e] *−1.5*[j]	*2.06(3)*, [h] *2.40(15)*[k]	*3.9(1)*, [e] *4.15(10)*[k]	
LDA	−9.62	−7.00	−1.21	1.46	3.36	7.55
LDA + GWA	−9.65	−7.13	−1.25	2.13	4.13	8.23
EXX	−9.29	−6.56	−1.08	2.36	3.99	8.91
EXX + GWA	−8.86	−6.62	−1.19	2.48	4.31	8.59

[a]Reference 34.
[b]Reference 35.
[c]Reference 43.
[d]Reference 44.
[e]Reference 45.
[f]Reference 46.
[g]Reference 47.
[h]Reference 48.
[i]Reference 49.
[j]Reference 50.
[k]Reference 51.
[l]Reference 52.
[m]Reference 53; gap at X.
[n]Estimated from Fig. 1 of Ref. 54.
[o]Estimated from Fig. 1 of Ref. 55.
[p]Reference 36.
[q]Reference 37.

for GaN. The corresponding shifts of the EXX(c) eigenvalues lead to EXX(c) band gaps that are larger than their LDA counterparts. The band gap increase is discussed in detail, for instance, in Ref. 11 and can also be inferred from Tables I–IX and Fig. 4.

B. Electronic structure

Table IX and Fig. 4 show that EXX(c)-based GWA calculations yield fundamental band gaps that are in very good agreement with experiment for all semiconductors studied here. While quasiparticle corrections for semiconductors whose EXX(c) band gap is already close to experiment are small, the quasiparticle correction is significant (0.8 eV) for diamond and necessary to obtain good agreement between theory and experiment. The accuracy of LDA-based quasiparticle calculations is comparable to the accuracy of EXX(c)-based quasiparticle calculations. This suggests that EXX(c)-based GWA calculations are an alternative to LDA-based GWA calculations which have the advantage of starting from physically more meaningful KS band structures. Note that the eight semiconductors chosen represent systems in which the LDA-based GWA approach works well and are therefore a challenging test for EXX(c)-based GWA calculations.

1. Medium-gap semiconductors

This subsection compares LDA, LDA-based GWA, EXX(c), and EXX(c)-based GWA results for the band structures of Si, Ge, GaAs, and AlAs with experiment. Among these four elements Si is special in the sense that core-relaxation and scalar- and fully relativistic effects decrease the LDA band gap by only 0.1 eV compared to a total reduction of about 1 eV in Ge and 0.9 eV in GaAs.[10] This indicates that the physics of the Si band structure is not complicated by relaxation and relativistic effects, which means that Si is a simple test case for theoretical calculations. For the same reason, performance assessment of a new technique cannot be limited to a calculation of Si alone.

TABLE II. Ge energies at high-symmetry points. Notation is the same as in Table I. All energies are in eV.

Method	Γ_{1v}	Γ'_{25v}	Γ'_{2c}	Γ_{15c}		
Expt. [a]	*−12.6,−12.9(2)*[b]	*0.00*	*0.90,0.89*[c]	*3.25(1),3.006,*[c] 3.206 [c]		
LDA	−12.74	0.00	−0.05	2.59		
LDA + GWA	−12.59	0.00	0.48	3.10		
EXX	−12.46	0.00	1.25	3.01		
EXX + GWA	−11.51	0.00	1.51	3.59		
	X_{1v}	X_{4v}	X_{1c}	X_{3c}		
Expt. [a]	*−9.3(2)*[b]	*−3.15(20)* *−3.5(2)*[b]	*1.3(2)*			
LDA	−8.88	−3.02	0.70	9.50		
LDA + GWA	−8.87	−3.08	1.15	10.04		
EXX	−8.56	−2.99	1.34	10.41		
EXX + GWA	−8.12	−3.08	1.30	11.19		
	L'_{2v}	L_{1v}	L'_{3v}	L_{1c}	L_{3c}	L'_{2c}
Expt. [a]	*−10.6(5)*	*−7.7(2)*	*−1.4(3)*	*0.744*	*4.3(2),4.2(1)*[d]	*7.8(6),7.9(1)*[d]
LDA	−10.67	−7.57	−1.37	0.12	3.77	7.07
LDA + GWA	−10.60	−7.63	−1.39	0.61	4.30	7.56
EXX	−10.37	−7.29	−1.36	0.99	4.22	7.96
EXX + GWA	−9.67	−7.09	−1.41	1.12	4.57	7.79

[a]Reference 56 unless otherwise noted.
[b]Reference 49.
[c]Reference 57.
[d]Reference 51.

Results for Si. As shown in Table I, the LDA, LDA-based GWA, EXX(c), and EXX(c)-based GWA Si valence band structures all fall within the range of observed experimental values. This agreement results from the large experimental uncertainties. Take the Γ_{1v} state as an example. Early experiments determine its location at -12.5 ± 0.6 eV (Ref. 34) and -12.4 ± 0.6 eV (Ref. 35), whereas more recent work finds a value of -11.4 eV (Ref. 36) and -11.2 eV (Ref. 37). The range of possible experimental values is about 2 eV or 15–20 % of the valence band width at Γ. Note that the accuracy of the commonly quoted experimental value of 12.5 ± 0.6 eV has been questioned recently.[38,39]

Comparison of the LDA and EXX(c) valence band energies shows that EXX(c) valence band widths are 0.1–0.4 eV smaller than their LDA counterparts. The addition of dynamical, nonlocal, and local field effects in the form of EXX(c)-based GWA calculations further decreases the valence band width by 0.2 to 0.7 eV. In contrast to LDA-based GWA calculations, the self-energy corrections to the lowest-lying valence band are substantial.

For the higher-lying, *p*-derived valence bands, the sign of the quasiparticle correction becomes negative. Again, EXX(c) *p* band widths are 0.1–0.4 eV smaller than their LDA counterparts. But in this case quasiparticle corrections increase the width of the EXX(c) *p* bands by about 0.1–0.2 eV.

For the Si conduction bands, the quasiparticle corrections to the EXX(c) band structure are generally a fraction (1/10–1/2) of the difference between the EXX(c) and LDA band structures. In contrast to LDA-based GWA calculations, EXX(c)-based GWA calculations give quasiparticle corrections that can be positive or negative. Also, these quasiparticle corrections show a strong state- and wave-vector-dependent dispersion (for example, the correction for L'_{2c} equals -0.32 eV and for X_{4c} 0.59 eV) rather than the ''scissors-shift'' behavior of LDA-based GWA calculations. Note that EXX(c)- and LDA-based quasiparticle calculations give energies that agree to within 0.1–0.4 eV for all conduction states with the exception of Γ'_{2c} (0.8 eV) and X_{4c} (1.0 eV).

Results for Ge, GaAs, and AlAs. Table II shows that in the case of Ge, discrepancies exist between EXX(c)-based GWA calculations and experiment. In particular, the lowest valence band at Γ, *X*, and *L* seems to be about 1 eV too high in energy. Part of this discrepancy may be due to experimental uncertainties as discussed in the case of Si and further experimental work may be necessary to clarify this point. Also, the lowest conduction band at Γ (*L*) is about 0.6 (0.4) eV too high in energy. This discrepancy results from the neglect of core polarization and relaxation effects in the present work. Shirley *et al.*[40] showed that these effects shift gaps in Ge by about 0.3 eV for LDA-based GWA calculations. Note that inclusion of spin-orbit effects in the theoretical data would further reduce the calculated band gaps by about 0.1 eV.

As in the case of Si, the valence band width is smaller in EXX(c) compared to LDA and the difference is increased

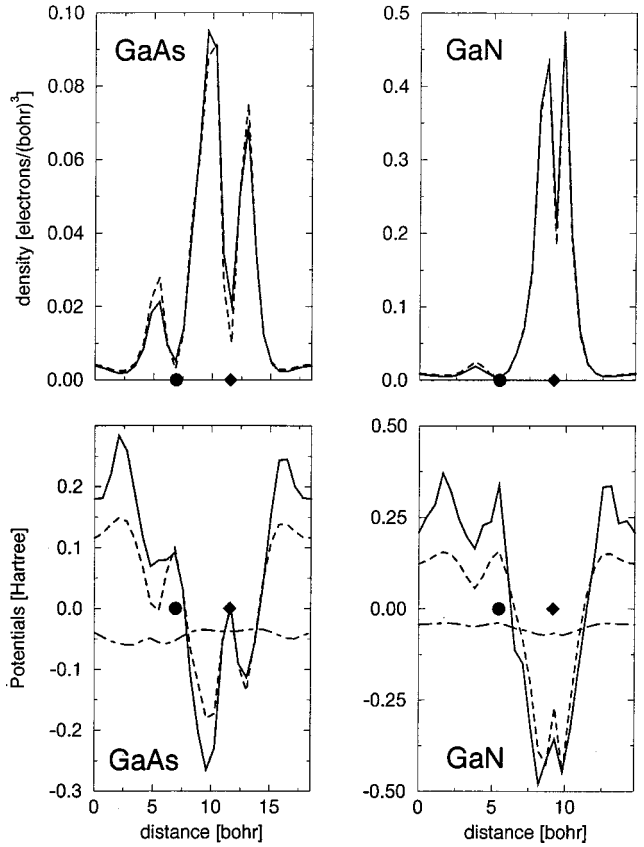

FIG. 3. Same as in Fig. 2 but for the heteropolar semiconductors GaAs (medium gap) and GaN (wide gap). The filled circle symbolizes the cation (Ga), the filled diamond the anion (As or N).

still more by quasiparticle corrections. Exactly the same observation holds for the GaAs and AlAs valence bands. Also, the conduction band quasiparticle corrections are qualitatively similar in Si, Ge, GaAs, and AlAs. We will therefore not discuss GaAs and AlAs in detail and limit ourselves to summarizing the results in Tables III and IV. To compare the GaAs and AlAs EXX(c)-based GWA calculations with experiment, note that core polarization and relaxation effects—omitted in the present study—affect low-lying conduction bands in GaAs (AlAs) by about 0.4 (0.2) eV (see Ref. 40).

The fact that the valence band width is smaller in EXX(c) than in LDA calculations is surprising at first sight. For example, in GaAs one would expect that the valence band minimum—which is predominantly cation *s*-like and more localized than the *p*-like valence band maximum—would be lowered with respect to the valence band maximum due to the elimination of self-interaction in EXX(c) compared to LDA.[29] This offset would produce a larger rather than a smaller bandwidth. However, the dominant factor seems to be a stronger electronic density localization in EXX(c) compared to LDA calculations, leading to an overall bandwidth narrowing.

2. Wide-gap semiconductors

The results for the band structures of the wide-gap materials C, SiC, GaN, and AlN are summarized in Tables V–IX and Fig. 4. Most of the qualitative points discussed for medium-gap semiconductors also apply for wide-gap semiconductors. The main qualitative difference between the wide-gap and medium-gap materials is the fact that the valence band width is generally larger in EXX(c) than in the

TABLE III. GaAs energies at high-symmetry points. Same notation as in Table I. All energies are given in eV. Spin-orbit splitting is neglected in the experimental data. Most of the experimental data are at room temperature.

Method	Γ_{1v}	Γ_{15v}	Γ_{1c}	Γ_{15c}		
Expt. [a]	*−13.21*	*0.00*	*1.52*	*4.61*		
LDA	−12.62	0.00	0.47	3.80		
LDA + GWA	−12.46	0.00	1.16	4.47		
EXX	−12.33	0.00	1.82	4.37		
EXX + GWA	−11.26	0.00	1.90	4.76		
	X_{1v}	X_{3v}	X_{5v}	X_{1c}	X_{3c}	X_{5c}
Expt. [a]	*−10.86*	*−6.81*	*−2.91*	*1.90*	*2.47*	
LDA	−10.29	−6.78	−2.57	1.42	1.62	10.19
LDA + GWA	−10.12	−6.98	−2.68	2.00	2.24	10.93
EXX	−10.02	−6.29	−2.48	2.15	2.31	11.20
EXX + GWA	−9.17	−6.36	−2.63	2.06	2.42	11.95
	L_{1v}	L_{1v}	L_{3v}	L_{1c}	L_{3c}	L_{1c}
Expt. [a]	*−11.35*	*−6.81*	*−1.41*	*1.74*	*5.45*[b]	*8.6*[b]
LDA	−11.01	−6.56	−1.09	0.97	4.68	7.74
LDA + GWA	−10.84	−6.74	−1.12	1.62	5.38	8.40
EXX	−10.72	−6.16	−1.04	1.94	5.19	8.71
EXX + GWA	−9.81	−6.24	−1.11	2.05	5.58	8.61

[a]Reference 58 unless noted otherwise.
[b]Reference 44.

TABLE IV. AlAs energies at high-symmetry points. Same notation as in Table I. All energies are in eV.

Method	Γ_{1v}	Γ_{15v}	Γ_{1c}	Γ_{15c}		
Expt. [a]		*0.00,−0.27*	*3.13*			
LDA	−11.89	0.00	1.87	4.22		
LDA + GWA	−11.51	0.00	2.74	5.06	9.43	10.04
EXX	−11.53	0.00	3.20	4.90		
EXX + GWA	−10.47	0.00	3.42	5.39		
	X_{1v}	X_{3v}	X_{5v}	X_{1c}	X_{3c}	X_{5c}
Expt. [a]			*−2.41*	*2.23*		
LDA	−9.92	−5.45	−2.18	1.32	2.17	10.19
LDA + GWA	−9.67	−5.55	−2.27	2.16	3.04	10.98
EXX	−9.59	−5.06	−2.02	2.26	2.93	11.38
EXX + GWA	−8.72	−5.30	−2.23	2.26	3.23	12.05
	L_{1v}	L_{1v}	L_{3v}	L_{1c}	L_{1c}	L_{3c}
Expt. [a]			$E_{L_{1c}}$ *−3.92*	*2.36*[b]		
LDA	−10.47	−5.60	−0.83	2.00	4.62	7.59
LDA + GWA	−10.19	−5.69	−0.87	2.84	5.52	8.46
EXX	−10.14	−5.19	−0.76	2.99	5.27	8.82
EXX + GWA	−9.22	−5.46	−0.85	3.27	5.75	8.87

[a]Reference 56 unless otherwise noted.
[b]Reference 59.

LDA for the former. Quasiparticle corrections to the EXX(c) band structure lower the energy of the lowest valence band even further. As a consequence, the theoretical bandwidth is about 1–2 eV larger than experiment.

Agreement between LDA- and EXX(c)-based GWA calculations is generally to within 0.1–0.7 eV. Occasionally, low- or high-energy states show differences of 1.0 eV or more. Note that differences in various LDA-based GWA calculations for wide-gap materials can also be as large as about 1 eV.[10]

TABLE V. Diamond (C) energies at high-symmetry points. Same notation as in Table I. All energies are in eV.

Method	Γ_{1v}	Γ'_{25v}	Γ_{15c}	Γ'_{2c}		
Expt. [a]	*−24.2±1,−21(1)* −23.0(2) [b]	*0.00*	*7.3*	*15.3(5)*[c]		
LDA	−21.35	0.00	5.58	13.10		
LDA + GWA	−22.88	0.00	7.63	14.54		
EXX	−21.51	0.00	6.28	13.96		
EXX + GWA	−22.01	0.00	7.74	15.11		
	X_{1v}	X_{4v}	X_{1c}	X_{4c}		
LDA	−12.61	−6.26	4.63	16.91		
LDA + GWA	−13.80	−6.69	6.30	19.50		
EXX	−12.76	−6.17	5.43	18.10		
EXX + GWA	−13.39	−6.52	6.21	20.42		
	L_{1v}	L_{1v}	L_{3v}	L_{1c}	L_{1c}	L_{3c}
Expt. [a]	*−15.2(3)*[c]	*−12.8(3)*[c]				*20±1.5*
LDA	−15.51	−13.33	−2.78	8.39	8.76	15.67
LDA + GWA	−16.95	−14.27	−2.98	10.63	10.23	18.14
EXX	−15.81	−13.14	−2.74	9.17	9.32	17.04
EXX + GWA	−16.45	−13.75	−2.91	10.77	10.40	18.41

[a]Reference 56 unless noted otherwise.
[b]Reference 60.
[c]Reference 61.

TABLE VI. Cubic SiC energies at high-symmetry points. Same notation as in Table I. All energies are given in eV. Experimental energies are deduced from the following transitions of Ref. 58 unless noted otherwise: X_{3c}-X_{1c}=3.10 eV, L_{3v}-X_{1c}=3.55 eV, X_{5v}-X_{1c}=6.0 eV, X_{5v}-X_{3c}=8.3 eV, L_{3v}-L_{3c}=9.7 eV, L_{3v}-L_{1c}=7.5 eV (from Ref. 62), Γ_{15c} = 7.75 eV, and X_{1c} = 2.39 eV.

Method	Γ_{1v}	Γ_{15v}	Γ_{1c}	Γ_{15c}		
Expt. [a]		*0.00*	*7.4* [b]	*7.75*		
LDA	−15.34	0.00	6.21	7.16		
LDA + GWA	−16.08	0.00	7.19	8.18		
EXX	−15.23	0.00	7.36	8.11		
EXX + GWA	−15.24	0.00	7.65	8.68		
	X_{1v}	X_{3v}	X_{5v}	X_{1c}	X_{3c}	X_{5c}
Expt. [a]		*−3.4*[b]		*2.39, 2.417*	*5.2(3)*	
LDA	−10.22	−7.82	−3.20	1.31	4.16	13.78
LDA + GWA	−10.96	−8.44	−3.53	2.19	5.23	15.23
EXX	−10.48	−7.41	−3.02	2.50	5.08	15.35
EXX + GWA	−10.65	−8.01	−3.44	2.32	5.46	16.34
	L_{1v}	L_{1v}	L_{3v}	L_{1c}	L_{3c}	L_{1c}
Expt. [a]			*−1.15*	*6.35*	*8.55*	
LDA	−11.71	−8.56	−1.06	5.33	7.12	9.90
LDA + GWA	−12.46	−9.19	−1.21	6.30	8.25	11.32
EXX	−11.85	−8.07	−1.01	6.30	8.07	11.45
EXX + GWA	−11.99	−8.77	−1.17	6.69	8.59	11.97

[a]Reference 58 unless otherwise noted.
[b]Reference 62.
[c]Reference 63.

TABLE VII. GaN energies at high-symmetry points. Same notation as in Table I. All energies are in eV. Reference 67 gives L_{3v}-L_{1c}=7.03 eV but does not determine the position of these levels with respect to the valence band maximum.

Method	Γ_{1v}	Γ_{15v}	Γ_{1c}	Γ_{15c}		
Expt.	*−12.5* [a]	*0.0*	*3.2* [b],*3.3* [c]			
LDA	−15.5	0.0	2.0	10.5		
LDA + GWA	−16.7	0.0	3.1	12.0		
EXX	−15.64	0.00	3.49	11.80		
EXX + GWA	−16.05	0.00	3.44	12.45		
	X_{1v}	X_{3v}	X_{5v}	X_{1c}	X_{3c}	X_{5c}
Expt.	*−11.85* [a]	*−6.1* [a]	*−2.0* [a]	*5.63* [d]		
LDA	−12.4	−6.1	−2.4	3.3	6.7	11.9
LDA + GWA	−13.5	−6.8	−2.7	4.4	8.1	14.0
EXX	−12.92	−5.53	−2.35	4.95	8.05	13.31
EXX + GWA	−13.27	−6.35	−2.71	4.54	8.50	14.68
	L_{1v}	L_{1v}	L_{3v}	L_{1c}	L_{1c}	L_{3c}
LDA	−13.2	−6.8	−0.8	4.8	8.9	10.5
LDA + GWA	−14.3	−7.6	−0.9	6.1	10.8	11.9
EXX	−13.59	−6.23	−0.84	6.24	10.52	11.79
EXX + GWA	−13.97	−7.17	−0.94	6.48	11.48	12.30

[a]Reference 64.
[b]Reference 65.
[c]Reference 66.
[d]Reference 67.

TABLE VIII. AlN energies at high-symmetry points. Same notation as in Table I. All energies are in eV. The experimental gap is 5.11 eV (Ref. 68).

Method	Γ_{1v}	Γ_{15v}	Γ_{1c}	Γ_{15c}		
LDA	−15.1	0.0	4.2	12.3		
LDA + GWA	−17.0	0.0	6.0	14.6		
EXX	−14.85	0.00	5.66	13.57		
EXX + GWA	−15.32	0.00	5.98	14.63		
	X_{1v}	X_{3v}	X_{5v}	X_{1c}	X_{1c}	X_{3c}
LDA	−12.3	−5.0	−1.8	3.2	8.4	14.1
LDA + GWA	−14.3	−5.6	−2.1	4.9	10.5	17.3
EXX	−12.45	−4.46	−1.63	5.03	9.69	15.40
EXX + GWA	−12.83	−5.29	−2.01	4.89	10.44	17.41
	L_{1v}	L_{1v}	L_{3v}	L_{1c}	L_{1c}	L_{3c}
LDA	−12.9	−6.0	−0.5	7.3	10.0	11.0
LDA + GWA	−14.9	−6.7	−0.6	9.3	12.6	13.2
EXX	−13.02	−5.24	−0.46	8.59	11.57	12.30
EXX + GWA	−13.44	−6.29	−0.55	9.23	12.71	13.13

IV. CONCLUSION

On the exact-exchange-plus-LDA-correlation level, Kohn-Sham band structures alone give a good description of the electronic structure of the *sp* bonded semiconductors Si, Ge, GaAs, AlAs, SiC, GaN, and AlN. EXX(c)-based GWA calculations for these systems lead to little changes in the fundamental band gaps and thus preserve the good agreement of theoretical and experimental data. The good agreement of EXX(c)-based GWA calculations with experiment and with LDA-based GWA calculations shows that EXX(c) wave functions and energies are good zeroth-order approximations for quasiparticle wave functions and energies.

While quasiparticle corrections are small for all materials with EXX(c) band gaps close to experiment, they are substantial (about 1 eV) for diamond. For diamond, a 0.7 eV discrepancy between the EXX(c) band gap and experiment is eliminated within EXX(c)-based GWA calculations. Note also that quasiparticle corrections are expected to be substantial and to lead to good agreement with experiment for solid hydrogen, Ne, and Ar. These materials are currently being studied[41] and they have EXX(c) band gaps that are smaller than experiment by a few eV.

TABLE IX. Summary table: calculated and experimental fundamental band gaps for eight semiconductors and insulators. All energies are in eV. For Si, the numbers refer to the Γ-X gap.

Material	LDA	LDA + GWA	EXX	EXX + GWA	Experiment
Ge	−0.05	0.48	0.99	1.12	0.74
Si	0.66	1.31	1.51	1.44	1.2
GaAs	0.47	1.16	1.82	1.90	1.52
AlAs	1.32	2.16	2.26	2.26	2.23
SiC	1.31	2.19	2.50	2.32	2.39,2.42
GaN	2.0	3.1	3.49	3.44	3.2,3.3
AlN	3.2	4.9	5.03	4.89	5.11
C	4.17	5.85	4.92	5.76	5.50

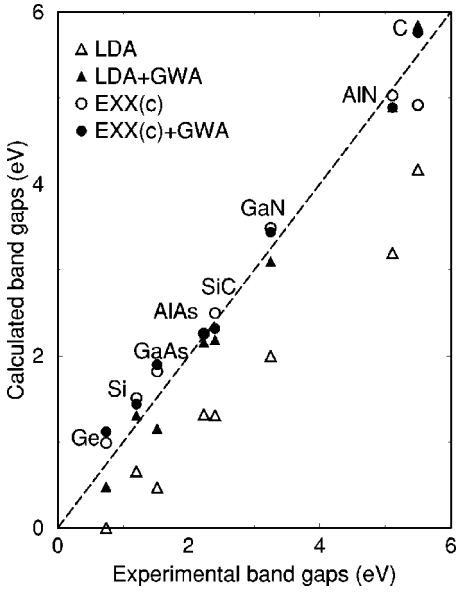

FIG. 4. Calculated fundamental band gaps in LDA (triangle), LDA-based GWA (filled triangle), EXX(c) (circle), and EXX(c)-based GWA (filled circle) in comparison with experiment for eight semiconductors. The dashed line indicates perfect agreement between theory and experiment. EXX(c)-based GWA calculations are as accurate as LDA-based GWA calculations, lead to only small corrections for materials whose EXX(c) band gap is close to experiment, and are essential to obtain agreement between theory and experiment in the case of diamond.

The valence band width of medium-gap semiconductors is generally 1–2 eV too small compared to experiment while the corresponding quantity for wide-gap semiconductors is 1–2 eV too large. While this discrepancy is in part caused by large experimental uncertainties for low-lying valence states, it may also be caused by the choice of LDA correlation in the EXX(c) calculations.

Since EXX(c) density functional calculations have only small self-interaction errors they potentially offer a better single-particle basis than the LDA for quasiparticle calculations of *d* and *f* electron systems. In particular, an EXX(c) basis should lead to good agreement between standard, non-self-consistent quasiparticle calculations and experiment for the energy eigenvalues of localized and delocalized electrons. Starting from a LDA basis, two separate calculations are required to describe, for instance, the electronic structure of CdS:[42] a non-self-consistent calculation for the band gap and a self-consistent calculation for the *d* electron level. A study of *d* and *f* electron systems within the EXX(c) and EXX(C) GWA approach will be the subject of future work.

ACKNOWLEDGMENTS

W.G.A. acknowledges helpful discussions with John Wilkins and support from the Ohio Supercomputer Center and the DOE under Contract No. DE-FG02-99ER45795. M.S. acknowledges financial support from the Office of Naval Research under Contract No. N0014-98-1-0594. A.G. acknowledges support from the Deutsche Forschungsgemeinschaft (Grant No. Go 523/5-2) and the Fonds der Chemischen Industrie.

[1] P. Hohenberg and W. Kohn, Phys. Rev. **136**, B864 (1964).
[2] W. Kohn and L. J. Sham, Phys. Rev. **140**, A1133 (1965).
[3] A. Görling, Phys. Rev. B **54**, 3912 (1996).
[4] C. Filippi, C. J. Umrigar, and X. Gonze, J. Chem. Phys. **107**, 9994 (1997).
[5] J. P. Perdew and M. Levy, Phys. Rev. Lett. **51**, 1884 (1983).
[6] L. J. Sham and M. Schlüter, Phys. Rev. Lett. **51**, 1888 (1983).
[7] R. W. Godby, M. Schlüter, and L. J. Sham, Phys. Rev. Lett. **56**, 2415 (1986); A. Schindlmayr and R. W. Godby, Phys. Rev. B **51**, 10 427 (1995).
[8] M. Lannoo, M. Schlüter, and L. J. Sham, Phys. Rev. B **32**, 3280 (1985); L. J. Sham, *ibid.* **32**, 3883 (1985); W. Knorr and R. W. Godby, Phys. Rev. Lett. **68**, 639 (1992).
[9] O. Gunnarsson and K. Schönhammer, Phys. Rev. Lett. **56**, 1968 (1986); **60**, 1582 (1988); K. Schönhammer and O. Gunnarsson, J. Phys. C **20**, 3675 (1987); K. Schönhammer, O. Gunnarsson, and R. M. Noack, Phys. Rev. B **52**, 2504 (1995).
[10] W. G. Aulbur, L. Jönsson, and J. W. Wilkins, Solid State Phys. **54**, 1 (1999).
[11] A. Görling, Phys. Rev. B **53**, 7024 (1996); **59**, 10 370(E) (1999); M. Städele, J. A. Majewski, P. Vogl, and A. Görling, Phys. Rev. Lett. **79**, 2089 (1997); M. Städele, M. Moukara, J. A. Majewski, P. Vogl, and A. Görling, Phys. Rev. B **59**, 10 031 (1999).
[12] T. Kotani, J. Phys.: Condens. Matter **10**, 9241 (1998); T. Kotani and H. Akai, Phys. Rev. B **54**, 16 502 (1996); **52**, 17 153 (1995); T. Kotani, Phys. Rev. Lett. **74**, 2989 (1995); Phys. Rev. B **50**, 14 816 (1994).
[13] D. M. Bylander and L. Kleinman, Phys. Rev. B **55**, 9432 (1997); **54**, 7891 (1996); **52**, 14 566 (1995).
[14] J. B. Krieger, Y. Li, and G. J. Iafrate, Phys. Rev. A **45**, 101 (1992); **46**, 5453 (1992); Y. Li, J. B. Krieger, and G.J. Iafrate, *ibid.* **47**, 165 (1993); R. T. Sharp and G. K. Horton, Phys. Rev. **90**, 317 (1953); J. D. Talman and W. F. Shadwick, Phys. Rev. A **14**, 36 (1976).
[15] F. Aryasetiawan and O. Gunnarsson, Rep. Prog. Phys. **61**, 237 (1998).
[16] We use an Engel-Farid plasmon pole model (see Ref. 21).
[17] Note that the only difference between the Kohn-Sham and Hartree-Fock exchange energies is that the latter quantity is calculated using Hartree-Fock rather than Kohn-Sham orbitals.
[18] For example, *d* and *f* electrons are underbound by 1–2 eV in the LDA.
[19] L. Hedin, Phys. Rev. **139**, A796 (1965).
[20] L. Hedin and S. Lundqvist, in *Solid State Physics*, edited by F. Seitz, D. Turnbull, and H. Ehrenreich (Academic, New York, 1969), Vol. 23, p. 1.
[21] G. E. Engel and B. Farid, Phys. Rev. B **47**, 15 931 (1993).
[22] S. L. Adler, Phys. Rev. **126**, 413 (1962).
[23] M. S. Hybertsen and S. G. Louie, Phys. Rev. B **35**, 5585 (1987).
[24] N. Wiser, Phys. Rev. **129**, 62 (1963).
[25] N. Troullier and J. L. Martins, Phys. Rev. B **43**, 8861 (1991); **43**, 1993 (1991); Solid State Commun. **74**, 613 (1990).
[26] L. Kleinman and D. M. Bylander, Phys. Rev. Lett. **48**, 1425 (1982).
[27] We have carried out extensive tests for both semilocal and separable pseudopotentials and found that typical differences in band gaps are on the order of 0.05–0.10 eV, which is only a few percent of their absolute values. Similar conclusions have also been noted in the literature [A. Dal Corso *et al.*, Phys. Rev. B **53**, 1180 (1996)].
[28] S. G. Louie, S. Froyen, and M. L. Cohen, Phys. Rev. B **26**, 1738 (1982).
[29] J. P. Perdew and A. Zunger, Phys. Rev. B **23**, 5048 (1981).
[30] D. M. Ceperley and B. I. Alder, Phys. Rev. Lett. **45**, 566 (1980).
[31] H. J. Monkhorst and J. D. Pack, Phys. Rev. B **13**, 5188 (1976).
[32] We use atomic units throughout this paper unless otherwise noted. In these units, energy is measured in hartree and $\hbar = e = m_e = 4\pi\varepsilon_0 = 1$ (ε_0 is the permittivity of vacuum).
[33] F. Gygi and A. Baldereschi, Phys. Rev. B **34**, 4405 (1986).
[34] L. Ley, S. P. Kowalcyzk, R. A. Pollak, and D. A. Shirley, Phys. Rev. Lett. **29**, 1088 (1972), as presented by J. R. Chelikowsky and M. L. Cohen, Phys. Rev. B **10**, 5095 (1974).
[35] W. D. Grobman and D. E. Eastman, Phys. Rev. Lett. **29**, 1508 (1972).
[36] D. H. Rich, T. Miller, G. E. Franklin, and T. C. Chiang, Phys. Rev. B **39**, 1438 (1989).
[37] J. R. Chelikowsky, T. J. Wagener, J. H. Weaver, and A. Jin, Phys. Rev. B **40**, 9644 (1989).
[38] R. Daling and W. van Haeringen, Phys. Rev. B **40**, 11 659 (1989).
[39] A. Fleszar (private communication).
[40] E. L. Shirley, X. Zhu, and S. G. Louie, Phys. Rev. B **56**, 6648 (1997).
[41] M. Städele and R. M. Martin, Phys. Rev. Lett. **84**, 6070 (2000).
[42] M. Rohlfing, P. Krüger, and J. Pollmann, Phys. Rev. B **56**, R7065 (1997).
[43] M. Welkowsky and R. Braunstein, Phys. Rev. B **5**, 497 (1972).
[44] J. E. Ortega and F. J. Himpsel, Phys. Rev. B **47**, 2130 (1993).
[45] W. E. Spicer and R. C. Eden, in *Proceedings of the Ninth International Conference on the Physics of Semiconductors, Moskau, 1968*, edited by S. M. Ryvkin (Nauka, Leningrad, 1968), Vol. 1, p. 61.
[46] D. E. Aspnes and A. A. Studna, Solid State Commun. **11**, 1375 (1972).
[47] Reference 43 as presented by F. Szmulowicz, Phys. Rev. B **23**, 1652 (1981).
[48] R. Hulthén and N. G. Nilsson, Solid State Commun. **18**, 1341 (1976).
[49] A. L. Wachs, T. Miller, T. C. Hsieh, A. P. Shapiro, and T.-C. Chiang, Phys. Rev. B **32**, 2326 (1985), as presented in Ref. 55.
[50] F. J. Himpsel, P. Heimann, and D. E. Eastman, Phys. Rev. B **24**, 2003 (1981).
[51] D. Straub, L. Ley, and F. J. Himpsel, Phys. Rev. Lett. **54**, 142 (1985).
[52] L. Steinbeck (private communication).
[53] R. W. Godby, M. Schlüter, and L. J. Sham, Phys. Rev. B **36**, 6497 (1987).
[54] M. Rohlfing, P. Krüger, and J. Pollmann, Phys. Rev. B **52**, 1905 (1995).
[55] M. S. Hybertsen and S. G. Louie, Phys. Rev. B **34**, 5390 (1986).
[56] *Numerical Data and Functional Relationships in Science and Technology*, edited by K.-H. Hellwege, O. Madelung, M. Schulz, and H. Weiss, Landolt-Börnstein, New Series, Group III, Vol. 17, Pt. a (Springer-Verlag, New York, 1982).
[57] D. E. Aspnes, Phys. Rev. B **12**, 2297 (1975).
[58] *Numerical Data and Functional Relationships in Science and Technology* (Ref. 56), Vol. 22, Pt. a.
[59] H. J. Lee, L. Y. Juravel, J. C. Wooley, and A. J. Springer-Thorpe, Phys. Rev. B **21**, 659 (1980).
[60] I. Jiménez, L. J. Terminello, D. G. J. Sutherland, J. A. Carlisle, E. L. Shirley, and F. J. Himpsel, Phys. Rev. B **56**, 7215 (1997).

[61] F. J. Himpsel, J. F. van der Veen, and D. E. Eastman, Phys. Rev. B **22**, 1967 (1980).
[62] W. R. L. Lambrecht, B. Segall, M. Yoganathan, W. Suttrop, R. P. Devaty, W. J. Choyke, J. A. Edmond, J. A. Powell, and M. Alouani, Phys. Rev. B **50**, 10 722 (1994).
[63] R. G. Humphreys, D. Bimberg, and W. J. Choyke, Solid State Commun. **39**, 163 (1981).
[64] S. A. Ding, G. Neuhold, J. H. Weaver, P. Häberle, K. Horn, O. Brandt, H. Yang, and K. Ploog, J. Vac. Sci. Technol. A **14**, 819 (1996).
[65] T. Lei, T. D. Moustakas, R. J. Graham, Y. He, and S. J. Berkowitz, J. Appl. Phys. **71**, 4933 (1992); T. Lei, M. Fanciulli, R. J. Molnar, T. D. Moustakas, R. J. Graham, and J. Scanlon, Appl. Phys. Lett. **59**, 944 (1992); C. R. Eddy, T. M. Moustakas, and J. Scanlon, J. Appl. Phys. **73**, 448 (1993).
[66] M. J. Paisley, Z. Sitar, J. B. Posthill, and R. F. Davis, J. Vac. Sci. Technol. A **7**, 701 (1989); Z. Sitar, M. J. Paisley, J. Ruan, J. W. Choyke, and R. F. Davis, J. Mater. Sci. Lett. **11**, 261 (1992).
[67] S. Logothetidis, J. Petalas, M. Cardona, and T. D. Moustakas, Mater. Sci. Eng., B **29**, 65 (1995).
[68] O. Ambacher (private communication).